Proceedings Paper:

Gowtham, K., Teeparthi, K. and Yadala, P.K. (2026) Transient Response Analysis in IBR-Dominated Power Systems Based on Short Circuit Ratio. In: 2025 11th International Conference on Power Systems (ICPS). 2025 11th International Conference on Power Systems (ICPS), 07-09 Dec 2025, Hyderabad, India. IEEE. ISBN: 979-8-3315-5600-6. ISSN: 2831-5529. EISSN: 2691-0233.

https://doi.org/10.1109/icps67276.2025.11364993

Transient Response Analysis in IBR-Dominated Power Systems Based on Short Circuit Ratio

Koduri Gowtham
Department of Electrical Engineering
National Institute of Technology
Andhra Pradesh, India
gowtham.koduri@gmail.com

Kiran Teeparthi
Department of Electrical Engineering
National Institute of Technology
Andhra Pradesh,India
kiran.t39@nitandhra.ac.in

Pavan Kumar Yadala
School of Electronics and Computer Science
University of Southampton
Southampton, UK
p.k.yadala@soton.ac.uk

***Abstract*—Inverter-based resources (IBRs) play a major role in transition to renewable energy, which poses new threats to the power grid's stability and dependability. As conventional synchronous generators are replaced by IBR causes decrease in the inertia of the grid. As the penetration level rises, the grid's strength decreases, making it more vulnerable to disturbances. This paper presents a dynamic performance evaluation of a grid-following inverter(GFLI) under varying grid strengths, characterized by different Short Circuit Ratios (SCRs). The inverter is designed with a constant DC voltage source, an L-filter interface, and a cascaded control structure that includes inner current control loops and outer power control (PQ) executed in the synchronous dq reference frame. The transient behavior and current tracking performance of the inverter are examined by applying a step change in active power reference from 10 kW to 11 kW. The Key system responses are observed by time-domain simulations. The analysis highlights the influence of grid strength on the Efficiency of the control strategy, especially in weak grid conditions. Results demonstrate that the proposed control strategy maintains stable operation and accurate power delivery under strong to moderately weak grid conditions, while performance degrades significantly under weak grid scenarios (SCR = 1).**

***Index Terms*—Short Circuit Ratio (SCR), Inverter-Based Resources (IBR), Phase Locked Loop (PLL), Grid Following Inverter(GFLI)**

I. Introduction

Due to growing concerns over global warming and environmental sustainability, the reliance on fossil fuels, particularly thermal-based power generation, has significantly declined [1].In response, the power sector is undergoing a major transition in the direction of clean, sustainable energy sources. This shift is predominantly enabled by IBR's, such as photovoltaic systems, Battery energy storage systems, and Wind turbines, which interface with the grid through power electronic converters [2]. Grid-connected inverters are designed to adapt to the behavior of the grid and supply power as required. GFLIs essentially act as current sources at their output terminals. They convert DC power from energy resources into AC power for the grid, with the primary goal of regulating energy exchange with the utility grid [3]. The output current's phase angle and magnitude are changed as part of the control strategy to adapt to grid events [4].One of their main features is the ability to establish frequency and voltage references by using an external voltage source. This implies that they are unable to operate independently or "black-start" a grid. [5]. The increasing adoption of sustainable energy sources poses substantial challenges to grid-connected inverters(GCIs) [4], High levels of renewable integration are often associated with intermittency,stochastic generation patterns,and frequent power fluctuations, all of which contribute to grid uncertainty. These dynamic conditions lead to variations in the number of photovoltaic systems and other inverter-based resources connected to the network. Consequently, grid-following inverters(GFLIs) often face operational challenges in weak grid environments. One major issue is the negative impedance characteristic induced by the phase-locked loop (PLL) [6], which can generate oscillations near the fundamental frequency due to insufficient damping [7]. In such conditions, the commonly used synchronous reference frame PLL (SRF-PLL) may struggle to maintain accurate phase tracking, leading to delayed synchronization and reduced accuracy [8]. Dynamic changes in grid impedance measured at the point of common coupling (PCC) lead to fluctuations in the Short Circuit Ratio (SCR), which directly affect system stability [9]. As SCR is a key indicator of grid strength, understanding its variability and addressing its effects are essential for providing steady and reliable operation in inverter-dominated power systems [10]. Most existing studies focus on small-signal analysis, impedance-based methods,or experimental validations of inverter behavior under weak grid conditions. However, there is limited work that provides detailed time-domain insights into the internal control dynamics of grid-following inverters across a range of SCR values. This study addresses that gap by using a control-level simulation model to evaluate the dynamic reaction of the inverter to different grid strengths. The main contributions of this work can be summarized as follows:

- A systematic assessment of inverter transient performance is conducted by the application of a step change in active power reference, revealing the control system's ability to respond under dynamic operating conditions.
- The impact of varying Short Circuit Ratios (SCRs) on inverter stability is thoroughly investigated, providing

979-8-3315-5599-3/25/$31.00 ©2025 IEEE

insights into system behavior under strong and weak grid scenarios.

- Extensive time-domain simulations are performed, and signals such as the Direct-axis voltage (v_d), Quadrature-axis voltage (v_q), Direct-axis current (i_d), Quadrature-axis current (i_q), Point of common coupling (PCC) voltage (v_{PCC}), PCC current(i_{PCC}), grid voltage (v_{grid}), and grid current (i_{grid}) are analyzed to highlight the challenges in synchronization and power quality under varying grid strengths.

The framework of the paper is as follows:In Section II, the system modeling and control scheme of the grid-following inverter are discussed.In Section III, the simulation results under varying SCR conditions are presented and summarized. Section IV concludes the work with key findings and future research directions.

II. METHODOLOGY

A. System Configuration

This section represents the mathematical modeling of a grid-following inverter (GFLI) system developed to assess its transient response under varying SCR's. The overall system configuration comprises a voltage source inverter (VSI), an L-type filter, a constant DC voltage source, and an equivalent Thevenin grid: ideal voltage source plus series inductive reactance as shown in Fig.1. The control architecture includes a SRF-PLL and a cascaded control loop consisting of an outer power (PQ) controller and an inner current controller operating in the dq frame.

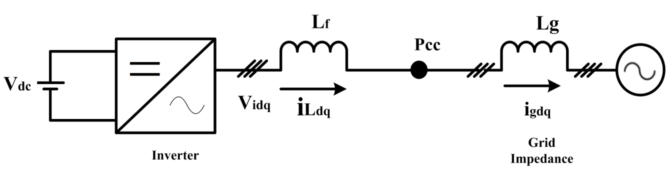

Fig. 1. Grid Following Inverter

B. Control Strategy

1) Park Transformation: The Park transformation converts three-phase quantities $\mathbf{V}_{pcc}$ into two orthogonal components $\mathbf{V}_{dq}$ in a synchronously rotating reference frame. This transformation aligns the d-axis with the instantaneous grid voltage vector, resulting in steady-state DC signals that simplify control implementation. It also facilitates decoupled control of active and reactive power via the d- and q-axis components, respectively. The transformation is illustrated in Fig.2a, and mathematically represented as:

$$V_d = \frac{2}{3}\left[V_a \cos(\theta) + V_b \cos\left(\theta - 120^\circ\right) + V_c \cos\left(\theta + 120^\circ\right)\right] \tag{1}$$

$$V_q = -\frac{2}{3}\left[V_a \sin(\theta) + V_b \sin\left(\theta - 120^\circ\right) + V_c \sin\left(\theta + 120^\circ\right)\right] \tag{2}$$

V_a, V_b, V_c are the three-phase instantaneous voltages,and θ is the instantaneous angle of the synchronous reference frame. This method is essential for vector control strategies and is widely used in inverter-based resource (IBR) systems

2) SRF-Phase Locked Loop: The utility networks and the grid-connected system are synchronized using the PLL. The function of PLL is used to measure the phase angle quickly and generate a reference signal for the grid-connected inverters. The PI controller is employed to control the quadrature-axis (v_q) voltage towards zero. This effectively synchronizes the reference frame with the phase angle of the grid voltage. Consequently, both the grid voltage amplitude (v_m) and frequency (f) can be extracted. The PLL's performance significantly influences the overall stability of the control system, particularly in weak grid environments or under voltage disturbances.The tracking of phase angle in fault conditions or weak grid conditions is not effective,which is analyzed for different SCR ratios. The framework for control of PLL is shown in Fig.2b

$$\omega(t) = \omega_0 + K_p^{\text{PLL}} v_q + K_i^{\text{PLL}} \int v_q dt \tag{3}$$

$$\theta(t) = \int \omega(t) dt \tag{4}$$

where $\omega(t)$ is instantaneous angular frequency, ω_0 is the nominal grid angular frequency, K_{p}^{PLL} and K_{i}^{PLL} are the proportional and integral gains of the PLL controller, respectively, and $\theta(t)$ is the estimated grid angle obtained by integrating the frequency.

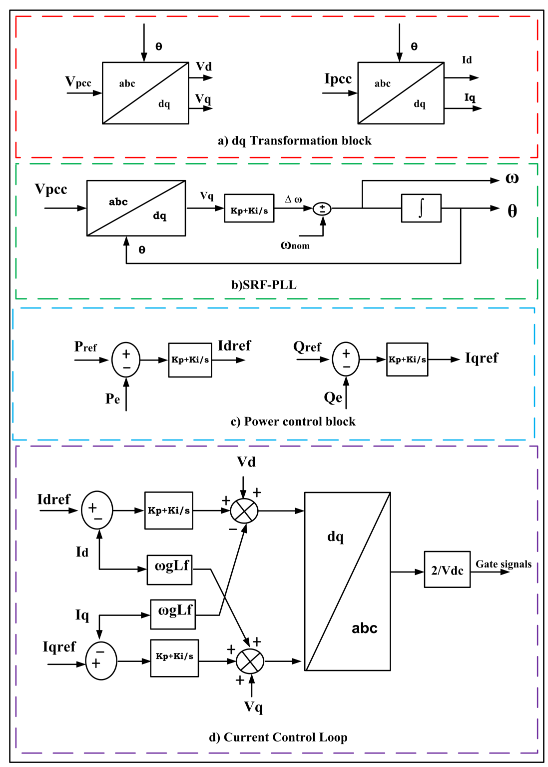

Fig. 2. Control structure of a grid-following inverter: (a) dq transformation block, (b) SRF-PLL, (c) Power control block, and (d) Current control loop

3) Power control Loop: In grid-following inverters, the outermost layer of control is the PQ control loop. It determines the values of reference for the d- and q-axis currents,denoted as I_d^{ref} and I_q^{ref}, which are passed to the inner current controllers. These references are derived from the instantaneous active and reactive power equations in the synchronous reference frame as:

$$P_{\text{rated}} = \frac{3}{2}(V_d I_d + V_q I_q) \tag{5}$$

$$Q_{\text{rated}} = \frac{3}{2}(V_q I_d - V_d I_q) \tag{6}$$

Assuming unity power factor operation ($i_q^{\text{ref}} = 0$, $v_q \approx 0$), the reference current is computed as:

$$i_d^{\text{ref}} = \frac{2}{3} \cdot \frac{P_{\text{ref}}}{v_d} \tag{7}$$

By setting appropriate values of P and Q, the control loop computes I_d^{ref} and I_q^{ref} accordingly, enabling decoupled regulation of active and reactive power flows with the grid.the control layer is shown in Fig.2c

4) Current control Loop: In GFLI, the Current Control loop acts as the fast inner loop responsible for regulating the output currents in the synchronous dq reference frame.The control structure for decoupled dq-axis current regulating The reference currents, I_d^{ref} and I_q^{ref}, generated by the outer power controller, are tracked by separate proportional-integral (PI) controllers. These controllers independently adjust the d- and q-axis currents to achieve accurate tracking.The resulting voltage references, E_d^{ref} and E_q^{ref}, are computed by the PI controllers while compensating for voltage drops across the filter inductance L and the inverter terminal voltage.Cross-coupling effects arising from the rotating reference frame are mitigated using feedforward decoupling terms. The control equations for the decoupled dq-axis PI current regulators are given as:

$$E_d^{\text{ref}} = V_d + K_p(I_d^{\text{ref}} - I_d) + K_i \int (I_d^{\text{ref}} - I_d)\, dt - \omega L I_q \tag{8}$$

$$E_q^{\text{ref}} = V_q + K_p(I_q^{\text{ref}} - I_q) + K_i \int (I_q^{\text{ref}} - I_q)\, dt + \omega L I_d \tag{9}$$

Here, K_p and K_i denote the gains of the PI controllers, ω is the angular frequency of the grid, and L is the filter inductance. The terms $\omega L I_q$ and $\omega L I_d$ represent the cross-coupling compensation in the d- and q-axes, respectively.The Fig.2d illustrates the control structure.

5) Inverter and Filter Dynamics: The inverter output current dynamics in the dq-frame, with an L-filter is given by:

$$\frac{di_d}{dt} = \frac{1}{L}\left(v_d^{\text{inv}} - v_d^{\text{PCC}} + \omega L i_q\right) \tag{10}$$

$$\frac{di_q}{dt} = \frac{1}{L}\left(v_q^{\text{inv}} - v_q^{\text{PCC}} - \omega L i_d\right) \tag{11}$$

These equations describe the coupling between the d and q components due to the rotating reference frame.The control structure shown in Fig.1.The system parameters used in this study are listed in tableI

TABLE I
SYSTEM PARAMETERS

Parameter (Symbol)	**Value**
Voltage (V_{grid})	415 V
Frequency (f)	50 Hz
DC Voltage Source (V_{dc})	800 V
Inverter Rating (S)	100 kVA
Switching Frequency (f_{sw})	10 kHz
Filter Inductance (L)	2.19 mH
K_p^{PLL}	5
K_i^{PLL}	1000
Current Controller Gain (K_p^i)	5
Current Controller Gain (K_i^i)	500

6) SCR Influence on Control Dynamics: SCR is a key metric used to assess the strength of the grid at PCC relative to the connected inverter. It is mathematically expressed as:

$$\text{SCR} = \frac{S_{\text{sc}}}{S_{\text{rated}}} = \frac{V_{\text{grid}}^2}{Z_{\text{grid}} \cdot S_{\text{rated}}} \tag{12}$$

Where S_{sc} Short-circuit strength of the grid at PCC, S_{rated} Rated apparent power of the inverter, V_{grid} RMS line-to-line grid voltage at PCC, Z_{grid} Equivalent Thevenin impedance of the grid.

where $Z_{\text{grid}} = j\omega L_g$ is the Equivalent grid impedance at the PCC. A low SCR indicates a weak grid with high impedance. In weak grid conditions, i.e, SCR < 3, the PCC voltage is more sensitive to current injection from the inverter. Across the grid impedance, the voltage drop is:

$$\Delta V = j\omega L_g \cdot I \tag{13}$$

This introduces phase errors and magnitude variations at the PCC, which directly impact the PLL's performance and Current controllers. The grid impedance and inductance calculated from the defined SCR levels are shown in the tableII

TABLE II
GRID IMPEDANCE AND INDUCTANCE VALUES DERIVED FROM SCR

SCR	**Inductance (mH)**	**Grid Impedance (Ω)**
10	0.5482	0.1722
9	0.6091	0.1914
8	0.6853	0.2153
7	0.7832	0.2460
6	0.9137	0.2878
5	1.0964	0.3445
4	1.3705	0.4306
3	1.8274	0.5741
2	2.7410	0.8611
1	5.4821	1.7223

III. SIMULATION RESULTS

Time-domain simulation results are shown in this section that illustrate the transient response of a GFLI under changing SCR conditions. Key control and system variables,including active and reactive power,dq-axis voltages and currents, phase angle, frequency, and waveforms at the inverter and PCC are analyzed to assess influence of Grid strength on inverter performance. The simulations reveal how SCR variations affect stability,power regulation and synchronization capabilities of the inverter.

A. *Active Power Response under Varying SCR Conditions*

Fig.3 shows the active power response of the GFLI under varying SCRs following a step change at $t = 1.5$ s. For strong grids (SCR = 4–10), the response is well-damped with minimal overshoot and fast settling, indicating effective control. At SCR = 3 and 2, oscillations with larger overshoot and slower settling appear, reflecting poor damping. At SCR = 1, the system becomes unstable with diverging power, caused by loss of synchronization and degraded current control. These results emphasize the adverse influence of weak grids and the importance of SCR in active power regulation.

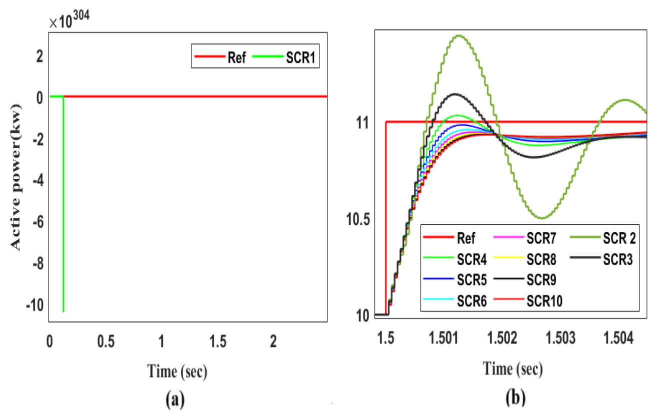

Fig. 3. Active Power Response under varying SCR Levels (1–10)

B. *Reactive Power Dynamics Under SCR Variations*

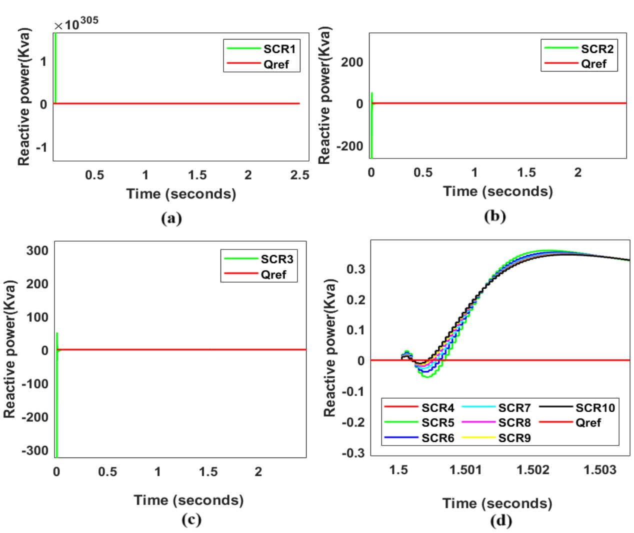

Fig. 4. Reactive Power Response under varying SCR Levels (1–10)

The Fig.4 illustrates the reactive power response of the grid-following inverter under varying SCR conditions following a change in active power in step. For SCR = 1, the system becomes numerically unstable, indicating a severe loss of control due to poor voltage support and PLL failure. At SCR = 2 and 3, significant oscillations are observed, starting with a negative dip followed by an overshoot, reflecting the strong coupling between active and reactive power dynamics in weak grids as shown in Fig.4. In contrast, for SCR Ranges from 4 to 10, the reactive power exhibits a well-damped transient with minimal deviation. As SCR increases, the magnitude of reactive power fluctuation decreases and the system settles faster.

C. *dq-Axis Voltage Response under SCR Variation*

The dq-axis voltage responses indicate the impact of SCR on voltage stability. For SCR = 1, unbounded voltage excursions are observed, revealing complete instability. For SCRs 2–3, oscillatory behavior in both $V_d$and $V_q$is present as shown in Fig.5, while SCRs greater than or equal to 4 shows stable tracking. Notably, Vq experiences a transient deviation due to the disturbance, with higher SCRs resulting in faster voltage recovery. The results highlight the strong dependence of voltage regulation and PLL synchronization on SCR as shown in Fig.5

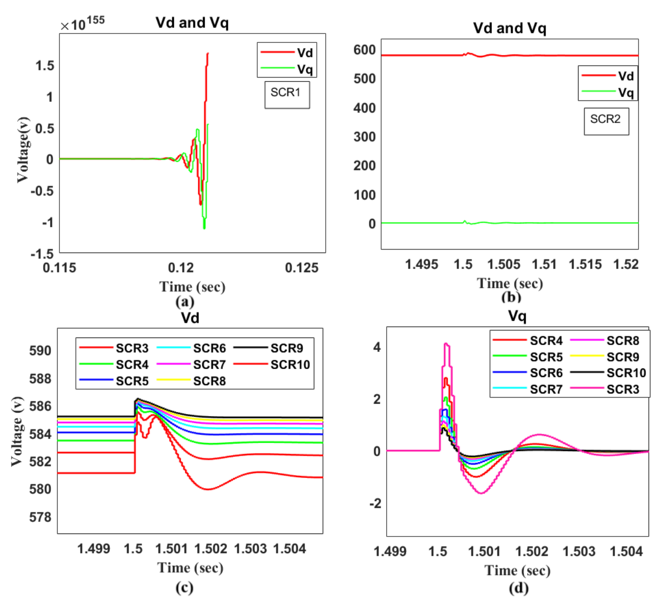

Fig. 5. dq-Axis Voltage Response under varying SCR Levels (1–10)

D. *Direct-Axis Current (I_d) Response and Reference Tracking*

The transient response of the direct-axis current (I_d) and its reference $I_d^{\mathbf{ref}}$ post active power step is depicted. Under weak grid conditions (SCR = 1,2,3), the current controller fails to track $I_d^{\mathbf{ref}}$, exhibiting large overshoot and poor damping. However, as the SCR increases beyond 4, the tracking improves significantly with reduced oscillations and faster settling. This indicates enhanced effectiveness of the inner current loop in stronger grids due to reduced grid impedance impact on control dynamics as shown in Fig.6

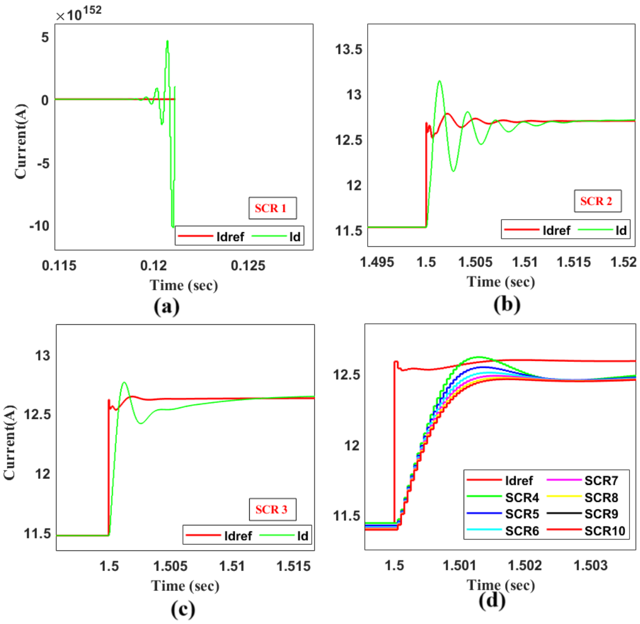

Fig. 6. Direct-Axis Current (I_d) Response under varying SCR Levels (1–10)

E. Quadrature-Axis Current (I_q) Response and Reference Tracking

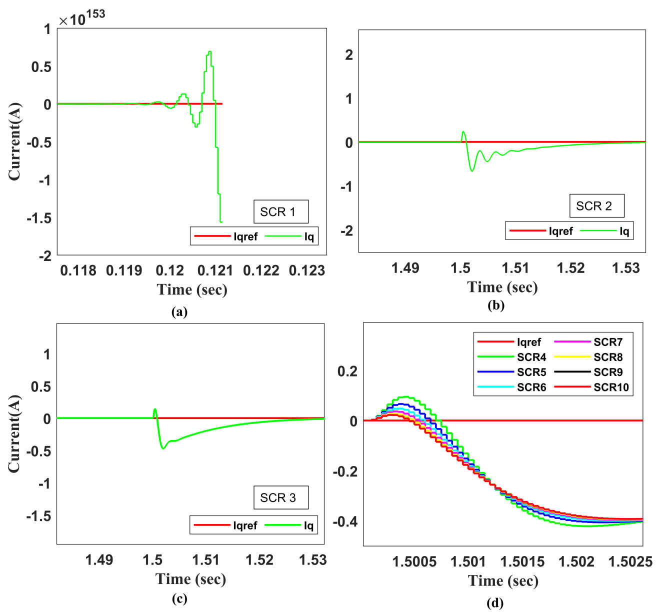

Fig. 7. Quadrature-Axis Current (I_q) Response under varying SCR Levels (1–10)

The inverter's I_q response shows transient reactive current injection immediately following the step in active power. Although $I_q^{\mathbf{ref}}$remains at zero, the system injects reactive current to support voltage recovery during the transient. At lower SCRs, especially SCR = 1, large instability is observed in I_q, indicating poor voltage regulation. Higher SCRs exhibit improved control, with I_q smoothly settling back to zero, demonstrating adequate decoupling of active and reactive power as shown in Fig.7

F. Frequency Response Following Active Power Step Change

This Fig.8 highlights the system frequency response across SCR values ranging from 1 to 10. The inverter becomes unstable at SCR = 1, showing diverging frequency, whereas SCR = 2 and 3 result in underdamped oscillations. From SCR = 4 onwards, the frequency stabilizes quickly with minimal deviation from nominal (50Hz), illustrating that adequate SCR levels are essential for maintaining frequency stability, particularly after abrupt changes in power demand.

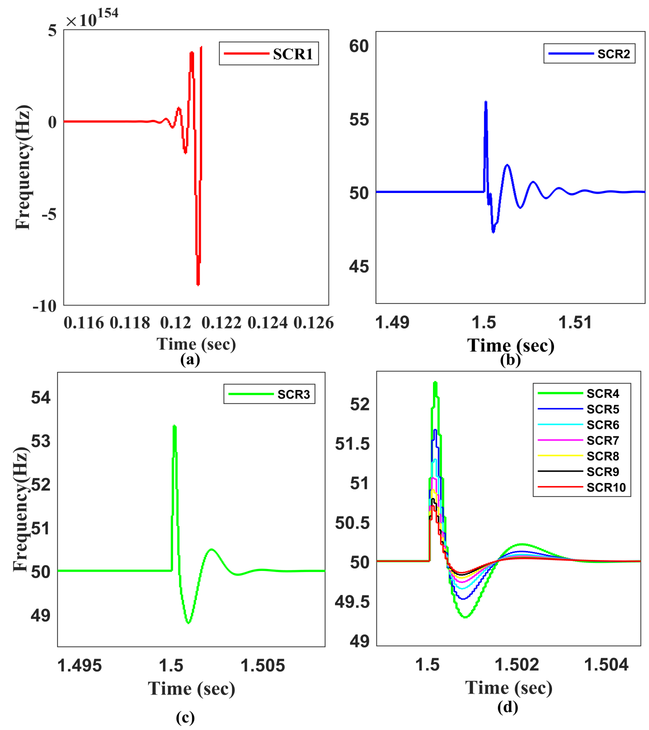

Fig. 8. Frequency tracking performance of the GFLI for varying SCR Levels (1–10)

G. Steady-State Voltage and Current at Inverter and PCC

Under strong grid conditions (SCR = 10), both inverter and PCC voltages remain stable and sinusoidal, with currents quickly settling after a power step change, as shown in Fig.10. The system demonstrates good dynamic performance with minimal transients. In contrast, Fig.9 shows that under weak grid conditions (SCR = 1), severe voltage and current oscillations occur, indicating poor damping and instability. These results highlight the critical impact of SCR on system stability and control effectiveness.

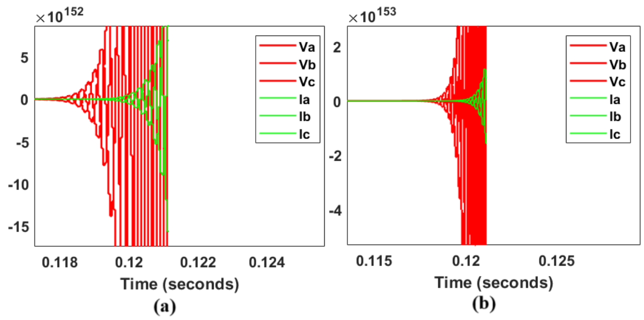

Fig. 9. Voltage and Current at PCC and Inverter a) SCR=1, b) SCR=2

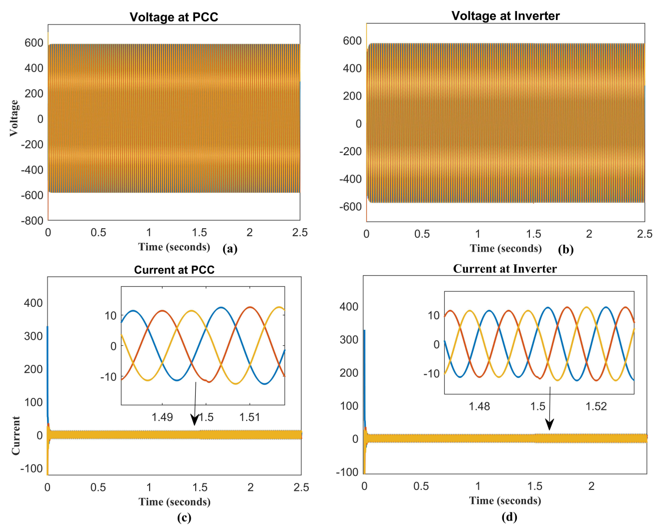

Fig. 10. Voltage and Current at Inverter and PCC for SCR=10

H. Phase Angle under Grid Disturbance

The estimated phase angle trajectory reflects the PLL's synchronization dynamics. For low SCRs, the slope of ωt changes more abruptly, showing a lag in phase tracking.High SCR cases show smooth and stable angle evolution, ensuring secure inverter-grid synchronization as shown in Fig.11

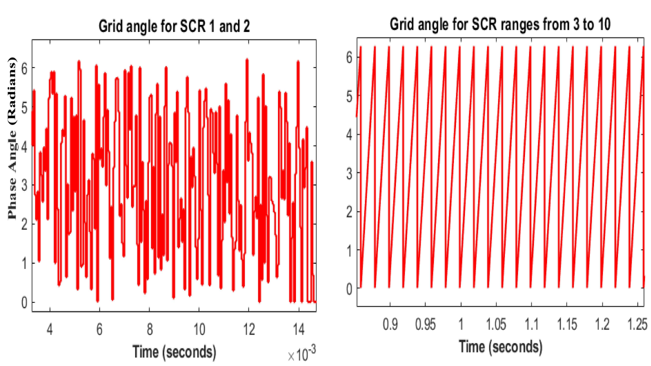

Fig. 11. Variation of phase angle tracking performance under different grid strengths

I. Consolidated Observations Under Varying SCR

The simulations confirms that grid strength strongly influences inverter performance. For SCR $\geq$ 4, responses are stable with accurate power tracking and smooth PLL operation. At SCR = 3, oscillations appear with slower synchronization, while SCR = 2 shows poor damping and weak PLL tracking. At SCR = 1, instability dominates with severe oscillations and complete PLL failure.

IV. Conclusion

This study showed that the SCR is a critical stability indicator for GFLIs using time-domain simulations. The results emphasize the operational limitations of GFLIs in low-inertia systems, while conventional PLL-based synchronization and current control strategies remain effective in strong grids, their performance degrades significantly as SCR decreases, leading to oscillatory or unstable dynamics. This work consolidates inverter behavior across SCR variations to establish a reference for stability boundary identification and control strategy development in IBR-dominated networks. Future work will extend this analysis to experimental validation and the development of advanced synchronization schemes, adaptive controller tuning, and grid-forming approaches to enhance efficiency in weak grid conditions.

References

[1] Y. Gu and T. C. Green, "Power system stability with a high penetration of inverter-based resources," *Proceedings of the IEEE*, vol. 111, no. 7, pp. 832–853, 2023.

[2] S. Prakash, O. A. Zaabi, R. K. Behera, K. A. Jaafari, K. A. Hosani, and U. R. Muduli, "Modeling and dynamic stability analysis of the grid-following inverter integrated with photovoltaics," *IEEE Journal of Emerging and Selected Topics in Power Electronics*, vol. 11, no. 4, pp. 3788–3802, 2023.

[3] Y. Li, Y. Gu, and T. C. Green, "Revisiting grid-forming and grid-following inverters: A duality theory," *IEEE Transactions on Power Systems*, vol. 37, no. 6, pp. 4541–4554, 2022.

[4] D. Lu, J. Yu, X. Lu, and J. Yu, "Synchronization stability of hybrid power systems integrated with grid-forming inverters and grid-following inverters," *CPSS Transactions on Power Electronics and Applications*, vol. 9, no. 4, pp. 405–415, 2024.

[5] W. Du, F. K. Tuffner, K. P. Schneider, R. H. Lasseter, J. Xie, Z. Chen, and B. Bhattarai, "Modeling of grid-forming and grid-following inverters for dynamic simulation of large-scale distribution systems," *IEEE Transactions on Power Delivery*, vol. 36, no. 4, pp. 2035–2045, 2021.

[6] J. Zhao, M. Huang, and X. Zha, "Nonlinear analysis of pll damping characteristics in weak-grid-tied inverters," *IEEE Transactions on Circuits and Systems II: Express Briefs*, vol. 67, no. 11, pp. 2752–2756, 2020.

[7] L. Huang, C. Wu, D. Zhou, and F. Blaabjerg, "A double-plls-based impedance reshaping method for extending stability range of grid-following inverter under weak grid," *IEEE Transactions on Power Electronics*, vol. 37, no. 4, pp. 4091–4104, 2022.

[8] H. Geng, L. Liu, and R. Li, "Synchronization and reactive current support of pmsg-based wind farm during severe grid fault," *IEEE Transactions on Sustainable Energy*, vol. 9, no. 4, pp. 1596–1604, 2018.

[9] C. Tu, J. Gao, F. Xiao, Q. Guo, and F. Jiang, "Stability analysis of the grid-connected inverter considering the asymmetric positive-feedback loops introduced by the pll in weak grids," *IEEE Transactions on Industrial Electronics*, vol. 69, no. 6, pp. 5793–5802, 2022.

[10] F. Han, X. Zhang, M. Li, F. Li, and W. Zhao, "Stability control for grid-connected inverters based on hybrid-mode of grid-following and grid-forming," *IEEE Transactions on Industrial Electronics*, vol. 71, no. 9, pp. 10 750–10 760, 2024.